GEOLOGIC MAP OF THE GRASSHOPPER JUNCTION 7 ½' QUADRANGLE, MOHAVE COUNTY, ARIZONA

by
Ferguson, C.A., Johnson, B.J.,
Pearthree, P.A. and Spencer, J.E.

October 2009

Arizona Geological Survey Digital Geologic Map 70
(DGM-70), version 1.0

Sheet 2 of 2

Citation for this map:
Ferguson, C.A., Johnson, B.J., Pearthree, P.A., Spencer, and J.E., 2009,
Geologic map of the Grasshopper Junction 7 ½' Quadrangle, Mohave County, Arizona
Arizona Geological Survey Digital Geologic Map DGM-70, version.1.0, scale 1:24,000, two sheets.

(Research supported by the U.S. Geological Survey, National Cooperative Geologic Mapping Program, under assistance award number 07HQAG0110. The views and conclusions contained in this document are those of the authors and should not be interpreted as necessarily representing the official policies, either expressed or implied, of the U.S. Government.)

Geochemistry

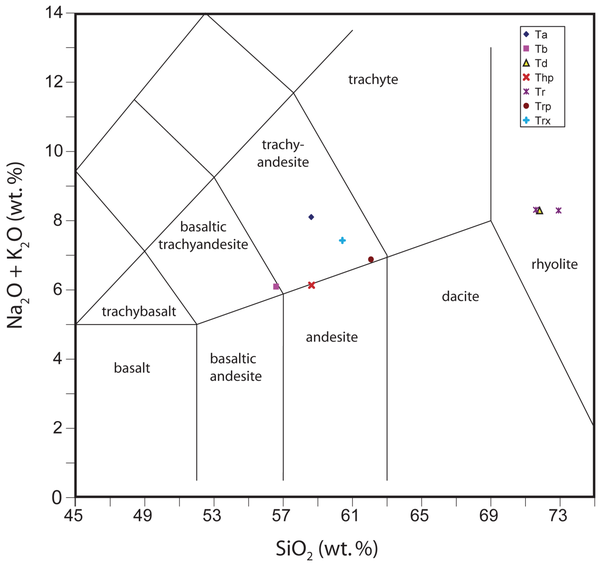

TABLE 1. MAJOR-ELEMENT CHEMISTRY

Sample number	map unit	SiO_2 (%)	Al_2O_3 (%)	Fe_2O_3(T) (%)	MnO (%)	MgO (%)	CaO (%)	Na_2O (%)	K_2O (%)	TiO_2 (%)	P_2O_5 (%)	LOI (%)	Total (%)	Ba (ppm)	Sr (ppm)	Y (ppm)	Sc (ppm)	Zr (ppm)	Be (ppm)	V (ppm)
21847	Ta	58.65	16.62	6.43	0.094	2.01	4.13	4.01	4.08	1.263	0.48	2.2	99.96	1596	744	27	11	312	2	108
22191	Tb	56.62	16.18	7.85	0.12	4.46	6.67	3.71	2.36	1.208	0.25	-0.16	99.26	579	378	28	19	212	2	128
21952	Td	71.84	13.07	1.48	0.041	0.24	1.05	3.02	5.26	0.221	0.05	3.34	99.61	861	139	20	3	161	2	9
22341	Thp	58.67	16.24	6.08	0.096	3.11	6.61	3.81	2.3	0.807	0.43	1.5	99.67	1172	786	22	11	265	2	101
21951	Tr	71.63	12.81	1.34	0.045	0.12	0.71	3.01	5.29	0.168	0.03	3.53	98.68	318	62	22	2	145	3	< 5
21954	Tr	72.94	12.81	1.52	0.042	0.25	1.06	3.05	5.23	0.223	0.04	3.84	101	848	135	20	3	176	3	9
21956	Trp	62.1	14.83	4.84	0.082	1.45	3.47	3.27	3.59	0.926	0.31	4.38	99.27	941	413	29	9	281	2	72
21964	Trx	60.45	15.89	5.38	0.077	2.17	4.6	3.61	3.8	0.837	0.3	2.48	99.59	1526	686	22	11	263	2	120
Detection Limit		0.01	0.01	0.01	0.001	0.01	0.01	0.01	0.01	0.001	0.01		0.01	2	2	1	1	2	1	5

All analyses by Activation Laboratories Ltd.
Sample preparation by lithium metaborate/tetraborate fusion. Analysis by inductively coupled plasma - mass spectrometry (Actlab whole-rock package code 4B (2008))

TABLE 2. GEOCHEMISTRY SAMPLE LOCATIONS

Area	sample number	GPS station	NAD	Grid zone	UTM East	UTM North
Grasshopper	21847	CAF-2-21847	83	11	742974	3918506
Grasshopper	21951	CAF-2-21951	83	11	738768	3917954
Grasshopper	21952	CAF-2-21952	83	11	738681	3917975
Grasshopper	21954	CAF-2-21954	83	11	738819	3917812
Grasshopper	21956	CAF-2-21956	83	11	738954	3917881
Grasshopper	21964	CAF-2-21964	83	11	739715	3917957
Grasshopper	22191	CAF-2-22191	83	11	738265	3920224
Grasshopper	22341	CAF-2-22341	83	11	743178	3920939

Structural Geology

Structural data: stereonet representation

Structural measurements of deformation fabrics in Paleoproterozoic rocks within the map area were plotted on stereonets using Rick Allmendinger's Stereonet software provided on his Cornell University website (www.geo.cornell.edu/geology/faculty/RWA/programs.html).

Measurements of foliation (n = 174) and lineation (n = 87) in Proterozoic crystalline rocks show a clear preferred orientation, with only one discernable population of foliations (Figures 3A, 3B, 3C) and lineations (Figures 3D, 3E, 3F) apparent on lower hemisphere stereonets. Both mylonitic and non-mylonitic foliation were identified, but these are gradational with each other. It appears most likely that shearing occurred during cooling so that early formed foliation and lineation were subject to much recrystallization, leading to non-mylonitic foliation, and later mylonitic foliation formed under cooler conditions where recrystallization was not as effective and grain size was substantially reduced during shearing.

At 22 locations where mylonitic foliation and lineation were measured, shear sense was also recorded from field observations of asymmetric petrofabrics (e.g., Simpson and Schmid, 1983; Lister and Snoke, 1984; Hanmer and Passchier, 1991). For some observations, lineation trend or plunge was calculated from foliation orientation, so lineation is plotted within foliation plane (Figures G, H, I). For other observations, lineation trend and plunge were measured independently from foliation strike and dip, so lineation is not necessarily plotted within the foliation plane.

Figure H plots all nine foliation and lineation measurements for which normal shear was recorded. Eigenvectors were calculated separately for both foliation and lineation, and are plotted (eigenvalues are also given). The eigenvector for lineations that represents the average lineation direction is plotted in figures H and I (green square "1" near center of stereonet H and on right side of stereonet I). The eigenvector that represents the average pole to foliations is also plotted (purple square "1" near northwest edge of stereonets H and I). The minimum and maximum principal stresses are assumed to lie mid-way between these two poles, and are marked "P" and "T" (for deviatoric "pressure" and "tension"). For normal shear pole "P" is more steeply plunging than pole "T" (Figure 3H). For reverse shear, pole "T" is more steeply plunging than pole "P" (Figure 3I).

Stereonet H (n = 9), with average lineation nearly vertical (green square "1" in Figure 3H) and "P" and "T" axes disposed symmetrically about the lineation pole, suggests dip slip on steeply southeast-dipping, northeast-striking shear zones (NW side up), whereas stereonet I (n = 13) indicates oblique (right-lateral) reverse slip on shear zones striking northeast and dipping southeast (SE side up).

We conclude that maximum pressure, as indicated by both stereonets H and I, was oriented between pole "P" in Figure H and pole "P" in figure I, and is thus moderately to gently dipping in the northwest quadrant (at about 25° 300°), while "T" is much more steeply plunging and is east of vertical. This indicates that shearing was dominantly in the reverse sense, with maximum compression approximately WNW-ESE. The oblique, right-lateral component of shearing is indicated in stereonet I by the location of the lineation cluster half way between pure dip slip and pure strike slip.

Previous structural geologic studies of the Cerbat Mountains (Duebendorfer et al., 2001, and references therein) identified two Paleoproterozoic penetrative deformations. The second deformation (D2) is dominant in Big Wash, directly southeast of the map area, but has affected rocks over much of the range. D_2 deformation was described as follows (Duebendorfer et al., 2001):

"The dominant fabric in the Cerbat Mountains is a northeast-striking, subvertical foliation (S_2)..." (p. 584).

"The presence of recrystallized quartz ribbons and dynamically recrystallized feldspar indicates that deformation occurred at minimum temperatures of 450°C, and the stability of garnet and hornblende in mylonites suggests even higher temperatures. Lineations within the D_2 mylonite zones plunge moderately to steeply east. Most mylonites record reverse shear sense with both northwest- and southeast-side-up kinematics (Fig. 8). A few mylonite zones record normal shear sense." (p. 584).

"Weak S-C fabrics indicate south-side-up, reverse-dextral kinematics." (p. 585).

We conclude that deformation fabrics recorded in the map area are part of the D_2 deformation episode identified by Duebendorfer et al. (2001). Their geochronologic studies constrained D_2 to between 1724 and 1680 Ma.

References Cited

Duebendorfer, E.M., Chamberlain, K.R., and Jones, C.S., 2001, Paleoproterozoic tectonic history of the Cerbat Mountains, northwestern Arizona: Implications for crustal assembly in the southwestern United States: Geological Society of America, v. 113, n. 5, p. 575-590.
Hanmer, S., and Passchier, C., 1991, Shear-sense indicators: A review: Geological Survey of Canada Paper 90-17, 72 p.
Lister, G.S., and Snoke, A.W., 1984, S-C mylonites: Journal of Structural Geology, v. 6, p. 617-638.
Simpson, C., and Schmid, S.M., 1983, An evaluation of criteria to deduce the sense of movement in sheared rocks: Geological Society of America Bulletin, v. 94, no. 11, p. 1281-1288.

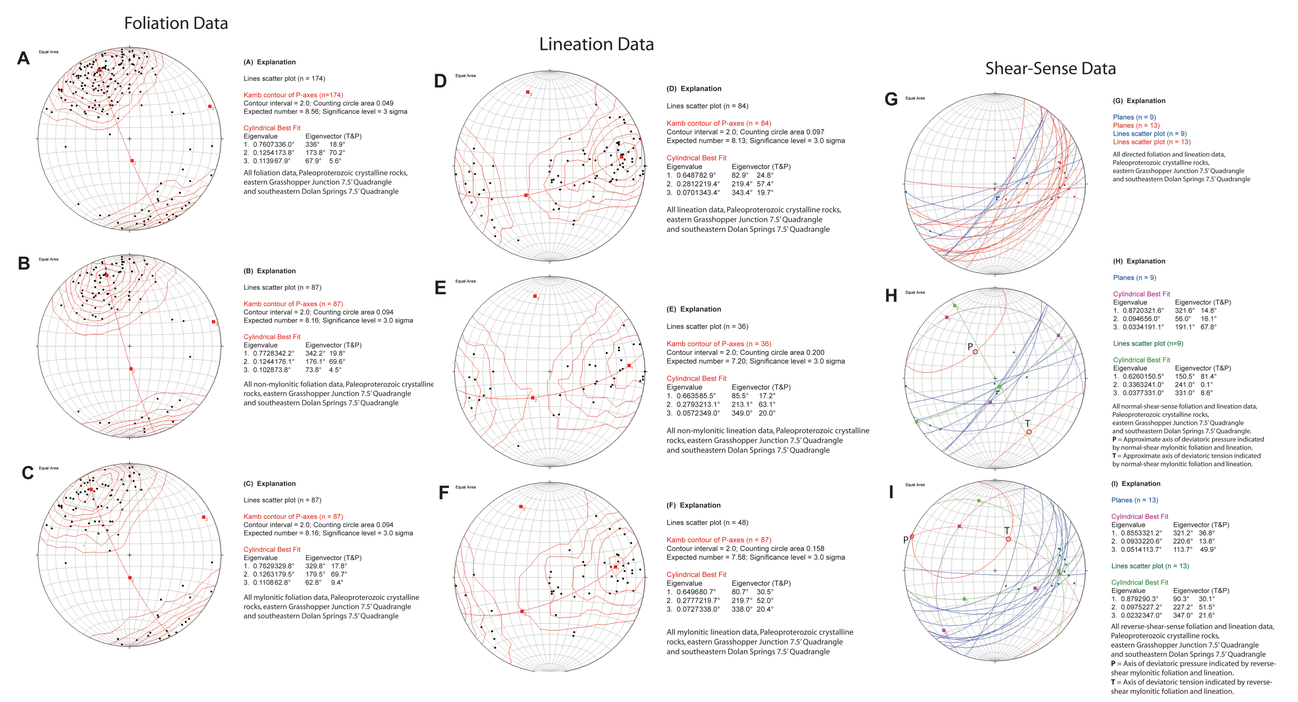
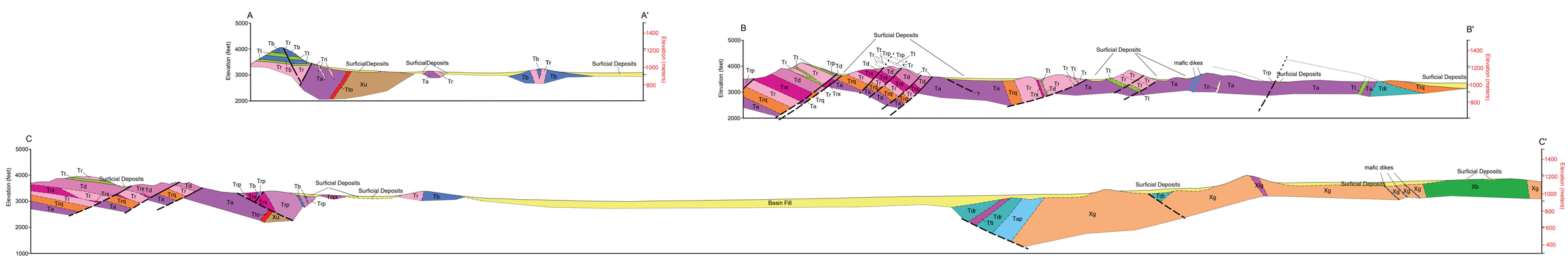
Cross Sections